We are IntechOpen, the world's leading publisher of Open Access books Built by scientists, for scientists

6,900
Open access books available

185,000
International authors and editors

200M
Downloads

Our authors are among the

154
Countries delivered to

TOP 1%
most cited scientists

12.2%
Contributors from top 500 universities

CLARIVATE ANALYTICS
BOOK CITATION INDEX
INDEXED

WEB OF SCIENCE™

Selection of our books indexed in the Book Citation Index
in Web of Science™ Core Collection (BKCI)

Interested in publishing with us?
Contact book.department@intechopen.com

Cumulative Tensile Damage and Consolidation Effects on Fracture Properties of Sandstone

Martin Šperl and Miloš Drdácký

Additional information is available at the end of the chapter

Abstract

The presence of cracks in many historical objects indicates the action of external forces accompanied by internal strain gradients. This is usually a repetitive process, and damage cumulation may occur. A study of these effects requires a suitable methodology for testing historical stone that has been subjected to repeated tension strains. The chapter presents the results of a pilot experimental assessment of changes in the mechanical characteristics of sandstone due to accumulation of damage. The Young modulus and the Poisson number were investigated, using a verified methodology for testing stone in simple tension and in cyclic simple tension/compression loading. The results show that the first tension load displacement can be approximated very satisfactorily by a power function, and the optical digital image correlation (DIC) method again demonstrated its capacity and suitability for measuring the complex deformation field on porous surfaces and on naturally well-structured surfaces. The chapter further presents a methodology for investigating fracture phenomena in sandstone treated for consolidation. It shows the preparation of test specimens with a cyclic loading generated crack, control of the test specimen preparation, and verification by means of X-ray micro-CT and DIC techniques. The chapter illustrates an influence of various consolidation agents on the toughness of cracked specimens.

Keywords: damage cumulation, sandstone, historical monuments, simple tension, cyclic loading, stone consolidation

1. Introduction

Visible cracks are present on most historical buildings, structures, and objects of art made of porous brittle or quasi-brittle materials. Stone monuments form an important category of these structures.

In principle, visible cracks may develop due to external forces acting under various time situations, for example, incidental shocks or gradually increasing loads, or due to internal strain gradients, which mostly generate cumulative damage, such as fatigue phenomena.

Cumulative tensile damage may occur in stone monuments due to repeated environmental uneven volumetric change. Stone objects are frequently subjected to repeated changes in temperature from solar irradiation, when the heat is transferred unevenly inside the material. The accompanying different thermal dilations may cause dangerous stresses that lead to cumulative crack propagation, typically initiated in the interior defects that are usually present. In addition, a combination of temperature and moisture dilation effects may worsen the situation, especially in sandstone or in specific fragile stones, e.g., in the so-called "opuka" stone (Cretaceous marly stone) used in the Czech Republic. In the case of these materials, stone elements in the interior environment are also threatened by environmental fatigue. Let us present a typical example that has been described in greater detail in Drdácký [1].

The second author of this paper investigated the case of a severe failure of the sandstone tracery of the triforium of St. Vitus Cathedral, where repeated uneven humidity loading (wetting and drying) and temperature loading (heating and cooling) were the cause of the collapse. A detailed survey discovered that this type of damage was present or had been repaired on most of the tracery arches of the triforium, where further failures subsequently occurred. The extent of the dangerous stresses was verified using simple thermal loading modeling and computations. It was proved that the state of stress in the damaged places reached or surpassed the material strength levels (**Figure 1**) [2].

The triforium tracery elements are chiseled out of a single piece of sandstone. They are connected with the lower window beam of the nave or the transept. The triforium structure is situated on the border between the exterior and the interior, and its ceiling plates are exposed to the exterior environment forming the roof structure. The temperature of the air fluctuates in the exterior and the interior of the cathedral. The stone elements of the triforium include parts of different proportions that have been composed into a single unit. Due to rapid changes in the ambient temperature, situations can arise when the temperature of the massive parts is different from the temperature of the subtler elements. This situation generates a stress inside
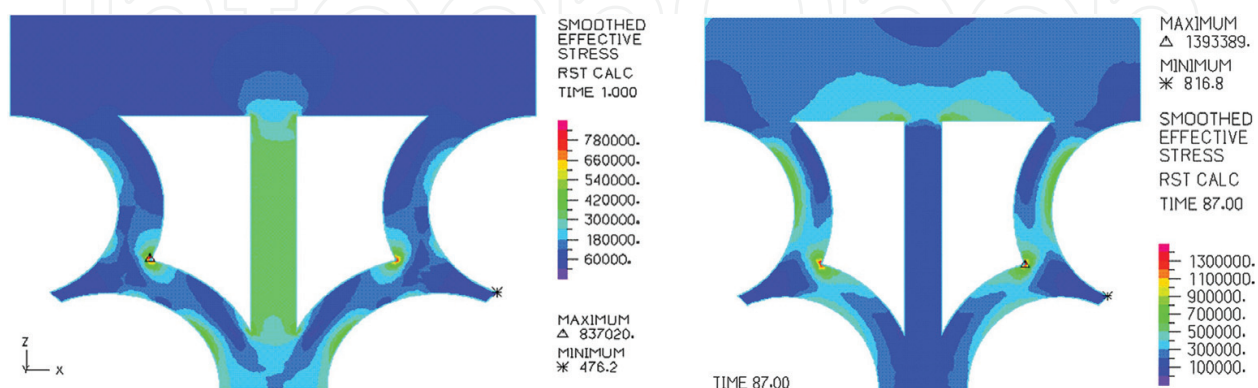
Figure 1. Distribution of the effective stress in the slice for coordinate y = 1.37; 3D model of own weight (left) and 3D model of warming up (right) [1, 2]. (Image by P. Beran).

the structure. The same effect is caused by the change in moisture content that always accompanies temperature changes.

Similar damage has been observed on other historic buildings, for example, on the church of Notre Dame du Sablon in Brussels (see **Figure 2**) where several failed original elements have been replaced.

Adverse effects of this type have led to a call for studies of the behavior of similar stone structures under extreme climate effects. These studies require greater knowledge than what is available of the fracture characteristics of the historical stone. Numerous works on the fracture behavior of rock have been published, mostly based on tests on cylindrical stone specimens under cyclic compression according to the ISRM standards (e.g., Ning et al. [3], Bagde and Petroš [4], Backers [5]). Quantitative toughness data are calculated, or qualitative data are assessed on the basis of these tests. A classical work by Attewell and Farmer [6] and also a comprehensive work by Jian-Qing et al. [7], which review fatigue damage variables and discuss a broad range of NDT measurement methods, in particular ultrasonic and acoustic emission methods, are worth mentioning. However, this type of testing methodology is not suitable for studies of the effects of conservation treatment on the fatigue behavior of stone. No pure tensile fatigue tests on stone have been found in the literature, only three-point or four-point bending tests (e.g., Cardani and Meda [8]). There is a lack of data on the behavior of stone under repeated uniaxial tensile loads, and until now no suitable methodology for testing stone toughness before and after conservation treatment has been suggested and accepted.

Figure 2. Repaired tracery with damaged elements in Notre Dame du Sablon (photo by M. Drdácký).

This paper presents the results of an experimental pilot assessment of changes in the mechanical properties of sandstone from Božanov (a typical material used on the Charles Bridge in medieval times) resulting from accumulated damage. The Young modulus and the Poisson number were observed. In addition, a methodology for testing stone in tension and in cyclic tension/compression loading is suggested and verified.

2. Experiments

Božanov stone is a grayish beige gross grain strong arkose sandstone without marked layering (**Figure 3**). The material used in the tests was extracted from the 11th arch of the Charles Bridge parapet wall, which had to be replaced during recent repairs. It has a rather deeply located detachment crack parallel to the surface, probably due to some previous surface treatment which had locked moisture inside the stone. The material can be characterized as a quasi-brittle inelastic silicate composite.

Test specimens $50 \times 50 \times 200$ mm^3 in dimensions were fixed into rectangular steel tubes with axially welded flat steel hangers, which served to fix the set into the hydraulic grips of the loading frame (**Figure 4**). Two-component Sikadur-31 CF RAP resin was used for gluing. The fixtures had to be prepared with great precision in order to ensure perfect alignment and perpendicular arrangement for tension and combined loading. The specimens in prismatic form were cut with negligible geometrical imperfections in a precise prismatic form.

The specimens were loaded into an Instron 1343 electrohydraulic testing frame with force capacity of 100 kN (**Figure 5**) using an Instron 100 kN load cell, a FastTrack 8800 controller, two Instron extensometers type 2620-602 (accuracy class 1, with maximum possible error of 0.5% of the read value, measurement base $l_0 = 50$ mm), and WaveMatrix measurement software. The extensometers were placed on opposite sides of the specimen, and their read values were arithmetically averaged. The contacts on the surface of the stone were provided with glued thin aluminum sheets to protect the extensometer wedges. The deformations were also

Figure 3. Macro photo of the Božanov sandstone (arkose) structure (photo J. Frankl).
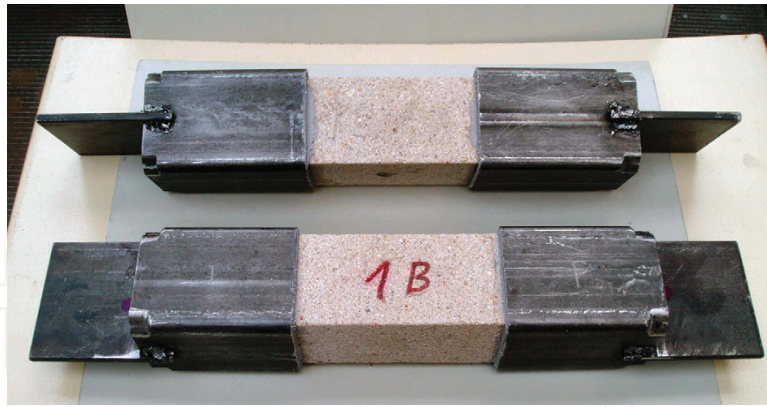
Figure 4. Test compression/tension specimens (photo by M. Šperl).
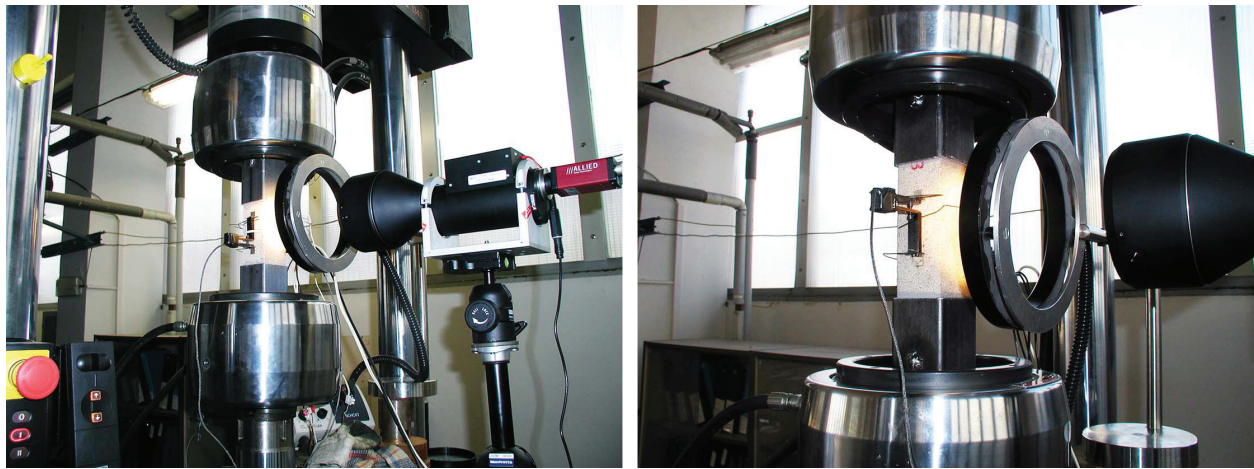
Figure 5. Arrangement of pure tension tests on the stone specimens (photo by M. Šperl).

recorded and evaluated using a contactless telecentric digital camera and the digital image correlation (DIC) method. This method utilizes a sequence of acquired images that represents a specimen surface deformation process. In this sequence, DIC observes the displacements of small rectangular regions (templates) on the sample with a distinguishable distribution of gray-scale intensities [9, 10]. The displacements obtained from this method are utilized for calculating the strains. In the case of stone, the random surface pattern, a prerequisite for the method, is formed by the distinct natural texture of the surface of the specimen.

The DIC algorithm used in this work has two main steps. First, an integer value of the pixel displacement is evaluated using a normalized cross-correlation function for a central pixel of a square image template in the reference image. The second step in the matching process is known as the Lucas-Kanade algorithm [11]. This step takes into account the reference template's own deformation. The method searches for an affine transformation that projects the template onto the deformed image using minimization of the sum-squared differences between the template and the deformed image. The LK algorithm is an iterative nonlinear optimization method. The integer values of the pixel displacement estimated in the first step

were passed to this iterative process as initial guess values. The longitudinal deformation was measured using two rows of points. Each point represents the center of the rectangular template, the displacement of which was measured by DIC. Multiple points were used, and their displacements were finally averaged for noise reduction. Subsequently, the longitudinal engineering strain was calculated using the measured displacements as

$$\varepsilon_{eng} = \frac{l - l_0}{l_0} \tag{1}$$

Knowing the measured applied force and the dimensions of the cross section of the specimen, the engineering stress can finally be evaluated.

Twelve experiments were carried out—four on the specimens from **Figure 4** and eight on prismatic beams cut out of the broken parts after the tension tests. The tests therefore involved (i) compression, (ii) very-low-cycle fatigue, (iii) tension, (iv) fatigue (an alternating nonsymmetrical cycle)—all on the specimens from **Figure 4**—and (v) three-point bending tests on small size beams with a 20×20 mm^2 cross section.

The effect of consolidation on the fracture behavior was studied on prismatic beams of the same cross section as described above provided in its center with a notch and a generated crack. The crack generation procedure is described in detail by Drdácký et al. [12]. Specimens with similar length of crack were consolidated applying the most typical agents: elastified Steinfestiger 300 (30% concentration of the active substance), Paraloid B-72 (2% concentration), and Funcosil 100 (10% concentration of the active substance). After maturing they were tested in standard static three-point bending.

3. Test results

The compression force was applied in three stages: -1.5, -26, and -37 MPa. Deformation was measured during the tests in order to study the change in Young's modulus and the Poisson number with relation to applied load (**Figures 6** and **7**). Hysteresis and irreversible deformation were observed, and the Poisson number reached a value of 0.23. The diagram shows that the tested sandstone increased in stiffness with an increasing number of compression cycles at the beginning of the tests. The change in the slope of the interpolated linear approximations of the load-displacement diagrams reflects this fact. The modulus of elasticity rose from an initial value of 11,360 MPa to a value of 19,237 MPa for the third cycle of loading, i.e., a 70% increase. This differs from the results of other tests on sandstone as presented in the cited literature. At the same time, hysteresis occurs with irreversible deformations. During the first loading cycle to -1.5 MPa, no irreversible deformation was observed. It seems that irreversible deformation occurs after the material has been subjected to some limit compression load. The Czech standard for tests on natural stone prescribes that the modulus of elasticity is to be evaluated after three loading cycles.

During the tension tests, the velocity of the crosshead movement was intentionally kept very low at a value of 5 μm/min. Due to this low loading velocity, it was possible to evaluate the overall energy absorbed during crack origin and propagation upon the initiation of a crack at a
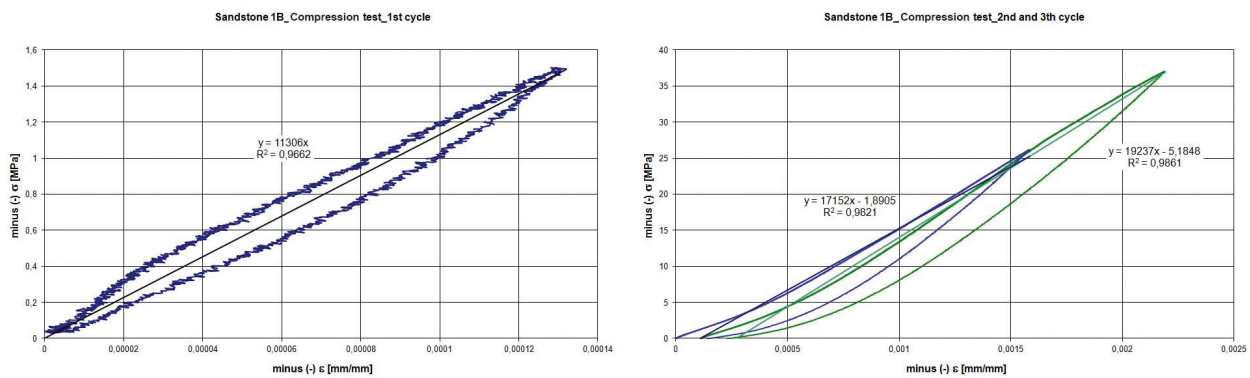
Figure 6 First compression loading cycle (left) and second and third loading cycles (right), with corresponding linear approximations.
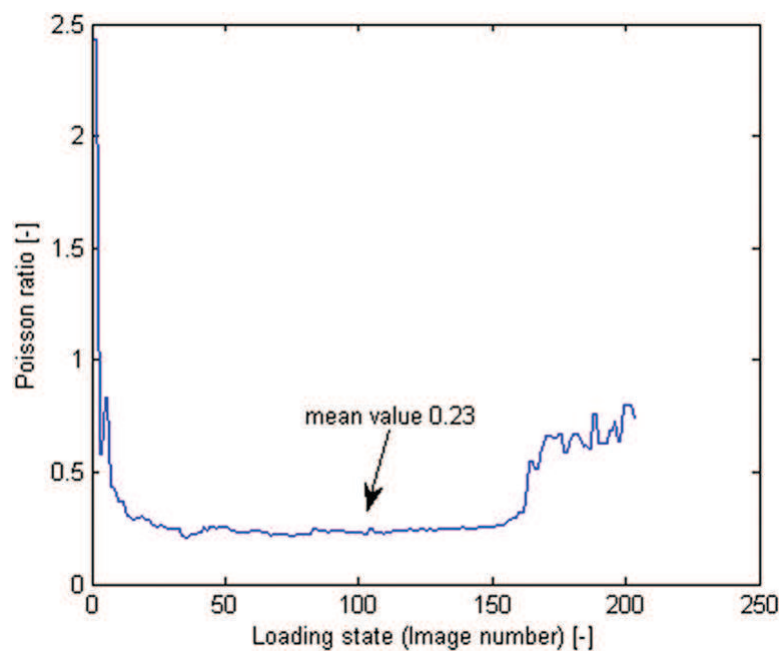
**Figure 7** Poisson ratio measured using the DIC method.

defect present within the specimen (**Figure 8**). The load-displacement graph shows the overall energy absorbed during the test (0.4 J) and during crack growth (0.16 J). This corresponds to the behavior of highly brittle material. The strength decreased (to 1.43 MPa) due to the defect in the material. The course of the stress and deformation up to fracture can be described well by means of a suitable power function (see **Figure 9**), which presents a detailed diagram.

It follows from **Figure 9** that a suitable power function appropriately describes the material behavior up to rupture. The tangent to the curve gives the modulus of elasticity value:
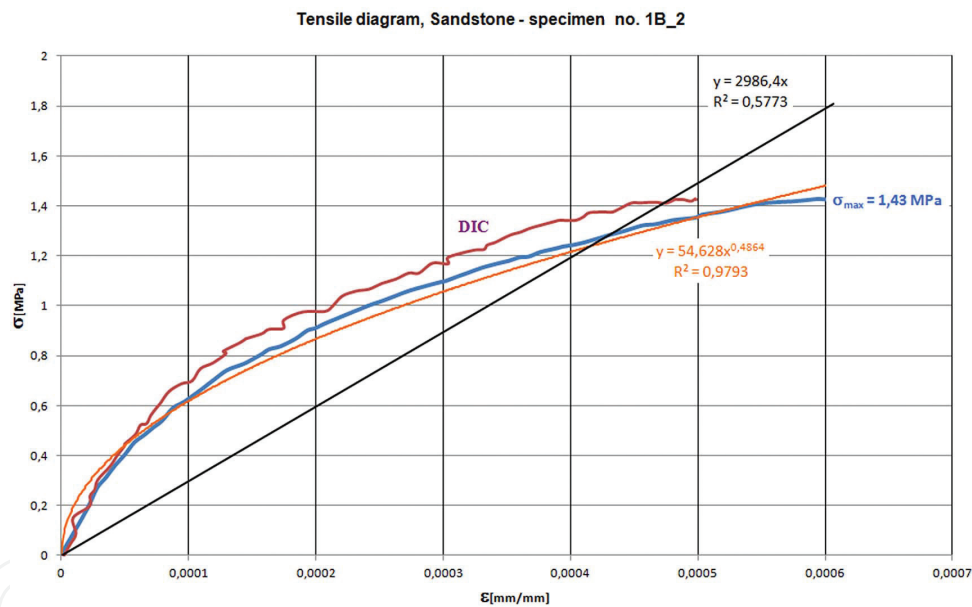
$$\sigma = k \cdot \varepsilon^{n} \quad \text{....by derivation after } \Sigma \text{ this yields:} \qquad E = \frac{d\sigma}{d\varepsilon} = k.n.\varepsilon^{n-1} \tag{2}$$

The power function seems to be ideal for describing the deformation behavior of this sandstone.
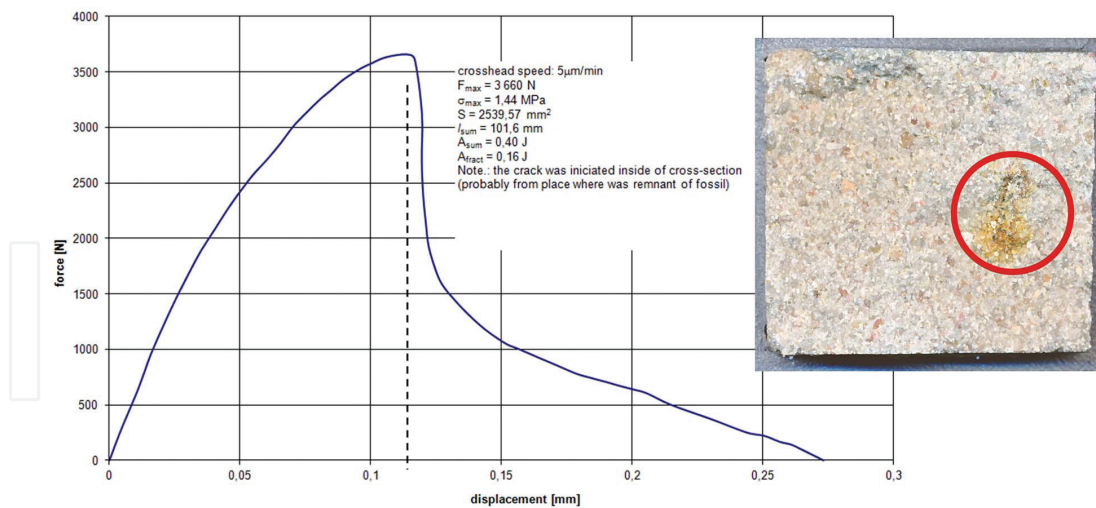
Figure 8. Load-crosshead displacement diagram for the tension test with a calculation of the absorbed energies and an indication of the probable place with an initial defect in the cross section of the specimen.

Figure 9. Tension diagram of the tested Božanov sandstone, comparing the conservative measurement with the DIC measurement and presenting a suitable power function approximation.

The DIC record exhibits a slight difference in comparison with the conservative measurement approach. This may be caused by a small change in the geometric relations between the specimen and the camera objective during loading. However, the agreement is still very good.

A sinusoidal altering nonsymmetrical loading cycle with stress limits of $+1.5$ and -2 MPa was applied during the very-low-fatigue test. The mean value of the stress was -0.25 MPa, the stress double amplitude was 3.5 MPa, and the frequency of loading was 0.2 Hz (**Figure 10**).
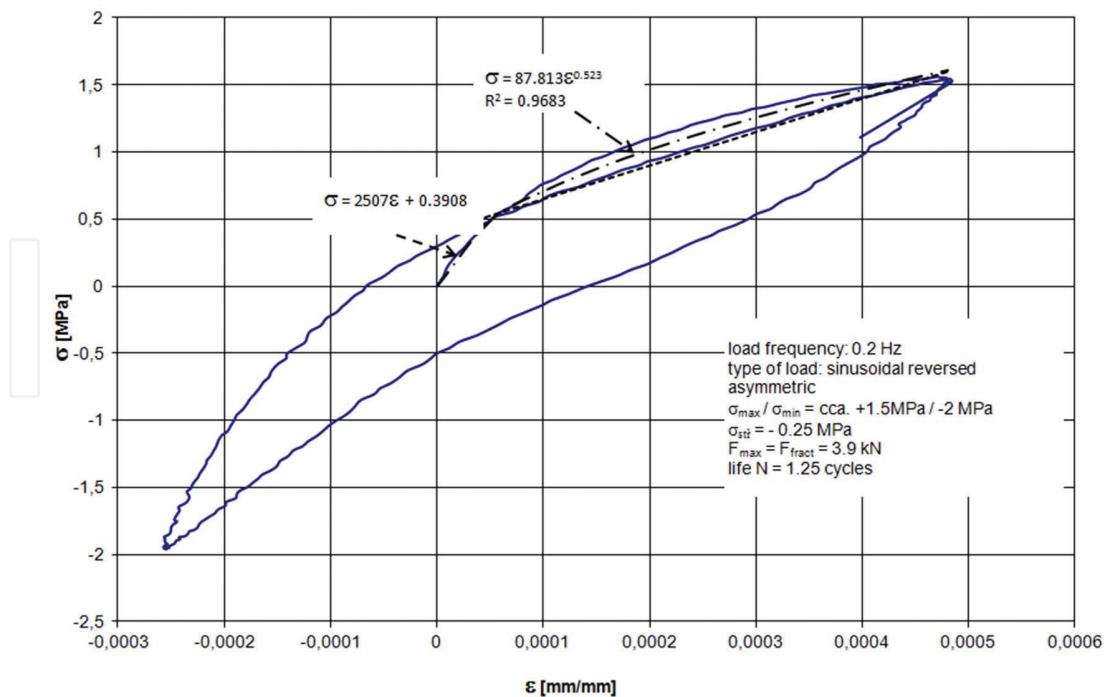
Figure 10. Low-cycle fatigue diagram.

The maximum tension stress ($\sigma_{max} \approx 1.5$ MPa) approached the limit stress (strength) in tension of the tested material (the static strength was 1.43 MPa on a weakened profile; see above). The resulting number of cycles was only 1.25; the fracture occurred while the maximum tension load was being attained in the second cycle.

Figure 10 also indicates that a power function can be used to approximate the first loading course. The parameters of the constant however are different from that of the previous case. This could be a result of the presence of an interior defect in the first case or merely the wide distribution of the material's characteristics. The change in the fatigue loop's tension branch is also noteworthy. In comparison to the first cycle, it is significantly straighter and more horizontal. It is even possible to approximate it with a linear function. It signifies considerable damage to the material resulting from the first loading cycle, corresponding to the stress applied. The hysteresis exhibited by this specimen is quite high. The compression component is steeper than the tension component [14].

The nonsymmetrical altering sinusoidal loading cycle was also used in the fatigue tests, with stress limits of +0.265 and −0.354 MPa. There were two modes of cycling velocity used—for the main loading sequence a frequency of 0.25 and 0.01 Hz at certain stages for groups of three cycles measuring deformations, based on which the second cycle was evaluated and the E modulus calculated. Such detailed measurements were attained up to 2000 cycles. The specimen was then loaded to the point of failure. The asymmetry characteristics of the cycle were kept the same to allow for comparability of results (R = −1.33 and stress span $\Delta\sigma = 0.619$ MPa). The overall lifespan reached 224,908 loading cycles. Typical results are presented in **Figure 11**.
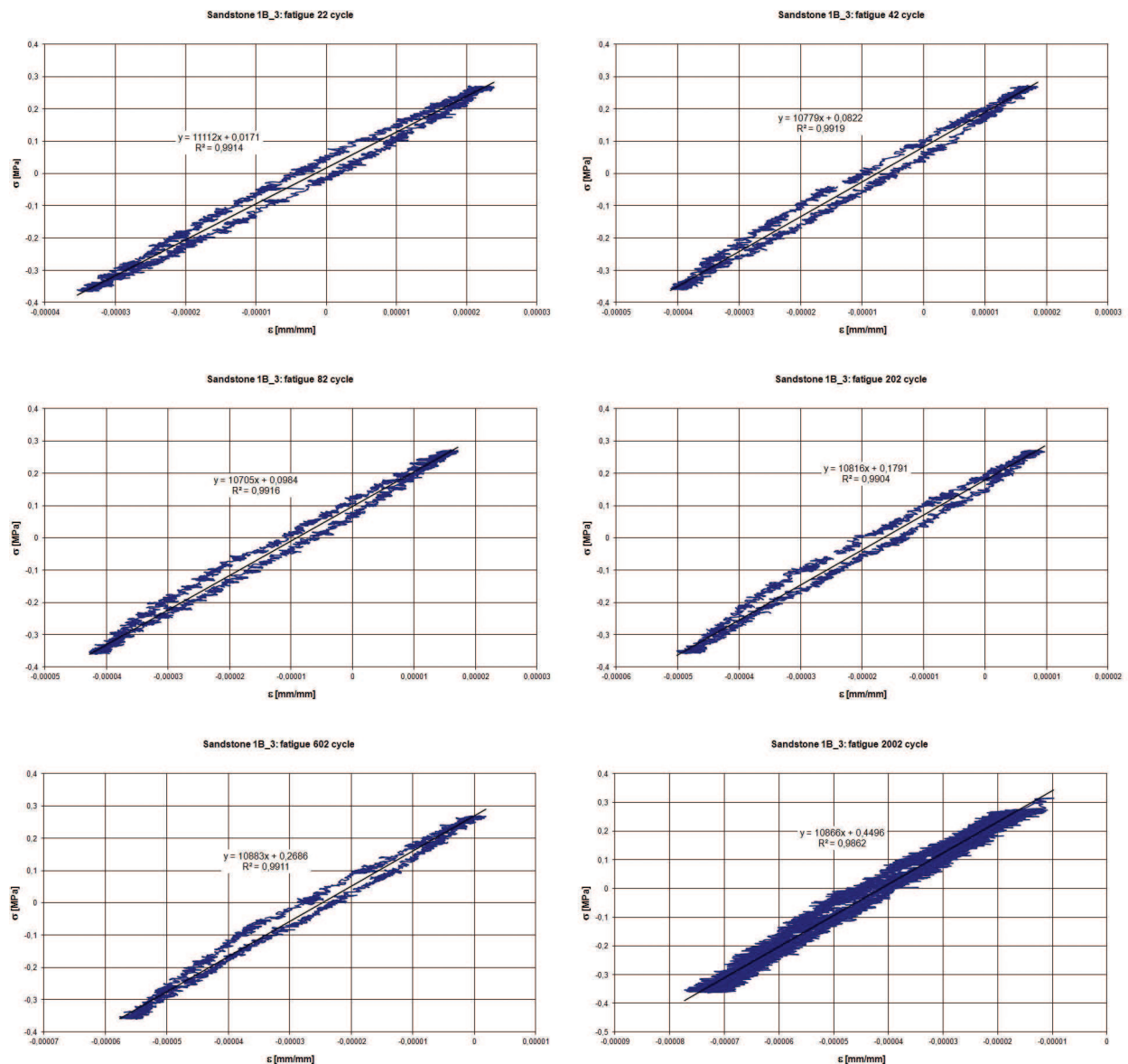
Figure 11. Stress-strain ratios after a given number of cycles: 22 (top left), 42 (top right), 82 (center left), 202 (center right), 602 (bottom left), and 2002 (bottom right).

The modulus of elasticity E changed during the cycling. Its value dropped from the initial figure of 11,214–10,705 MPa after 82 loading cycles (a decrease of about 5%). Then the value stabilized around 10,865 MPa after 2002 cycles (**Figure 12**). The change was influenced by fatigue damage in the material.

In **Figure 11**, the observed shift of the measured data toward negative strain values with the increasing number of cycles is caused by thermal dilation of the specimens. The average change in temperature in the testing hall was about 4°C. The temperature change dilations were checked by computations, taking into account the coefficient of dilation of sandstone equal to $\alpha = 10 \times 10^{-6}$ K^{-1} and the equation $\Delta l = \alpha \cdot \Delta T \cdot l$. **Figure 13** presents examples of the temperature drift.
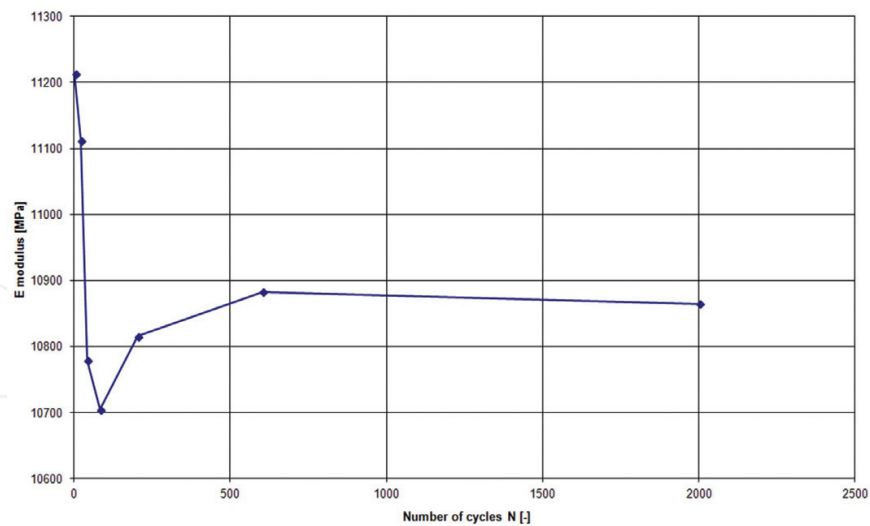
**Figure 12.** Change in the modulus of elasticity during cycling.
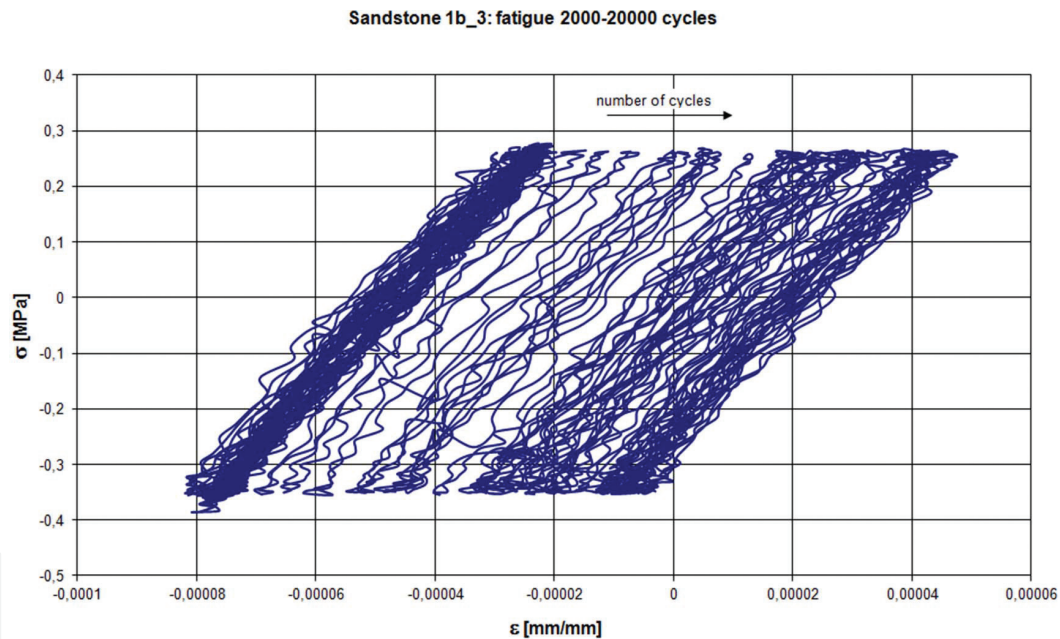
Figure 13. Temperature caused a drift in specimen deformation due to dilation (2000–20,000 cycles).

Figure 14 presents a very rough representation of the probable life estimate of the tested sandstone between two applied stress levels. Of course, many more tests will be required before the true Wöhler curve can be constructed.

After the uniaxial and fatigue tests, small beams with a cross section of 20×20 mm^2 were prepared from the broken specimens and were subjected to three-point bending loading (**Figure 15**). The measured flexural strength reached much higher values (about 4.5 MPa) than the strength in the tension tests, which was influenced by a rather low span to height ratio (about 3.75).
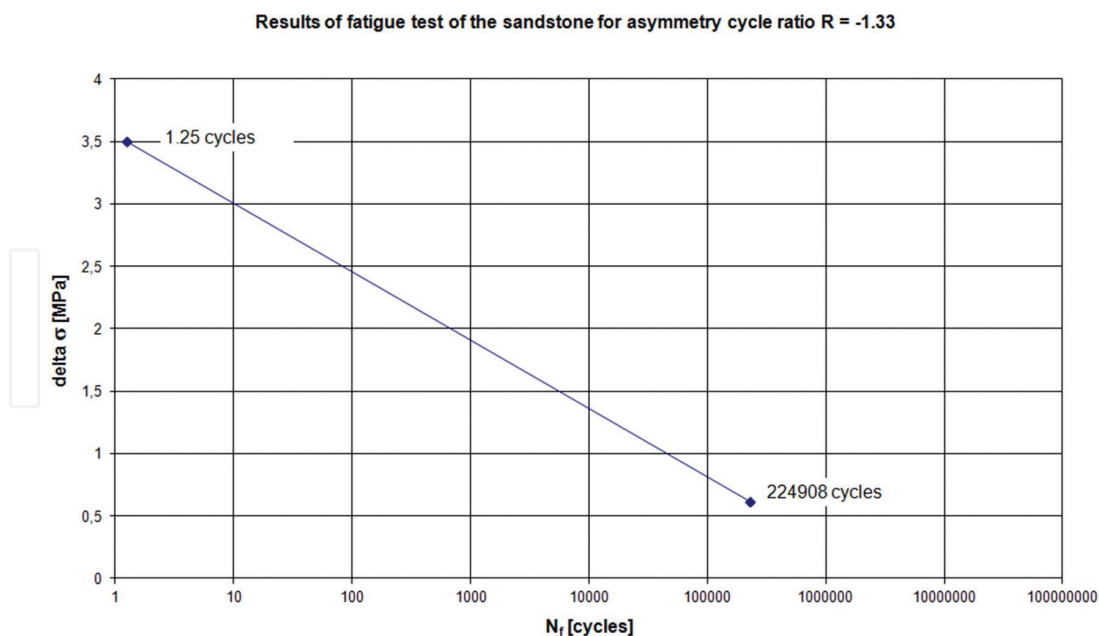
Figure 14. Fatigue test results for Božanov sandstone for cycle asymmetry of R = −1.33.
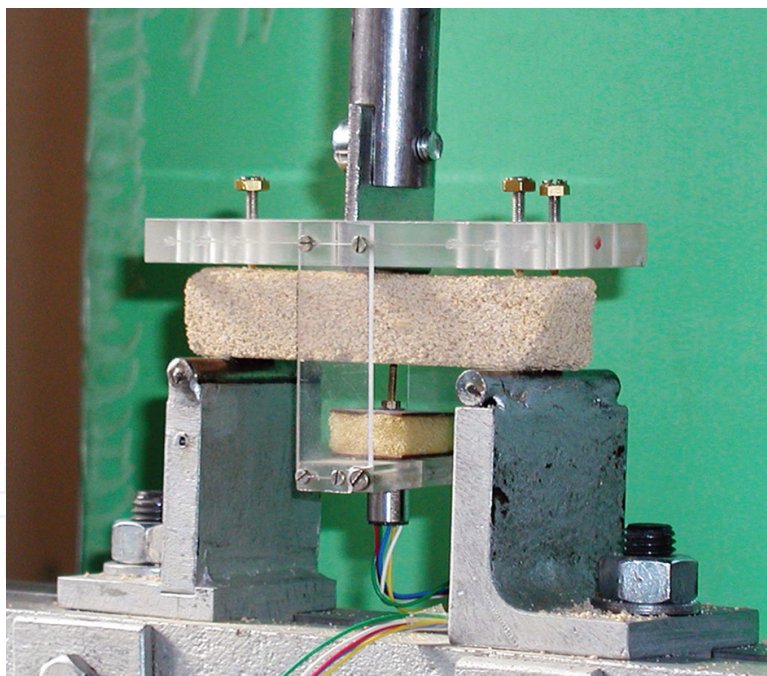
Figure 15. Three-point bending test arrangement (photo O. Vála).

However, the moduli of elasticity were lower than those measured during the previous tests (though still higher than those measured by the first author on thin plates during tests on the characteristics of the Charles Bridge sandstone—Čechová et al. [13]). It is clear that both the load-displacement diagram and the change in the modulus of elasticity can be well approximated by a suitable mathematical model (**Figure 16**).
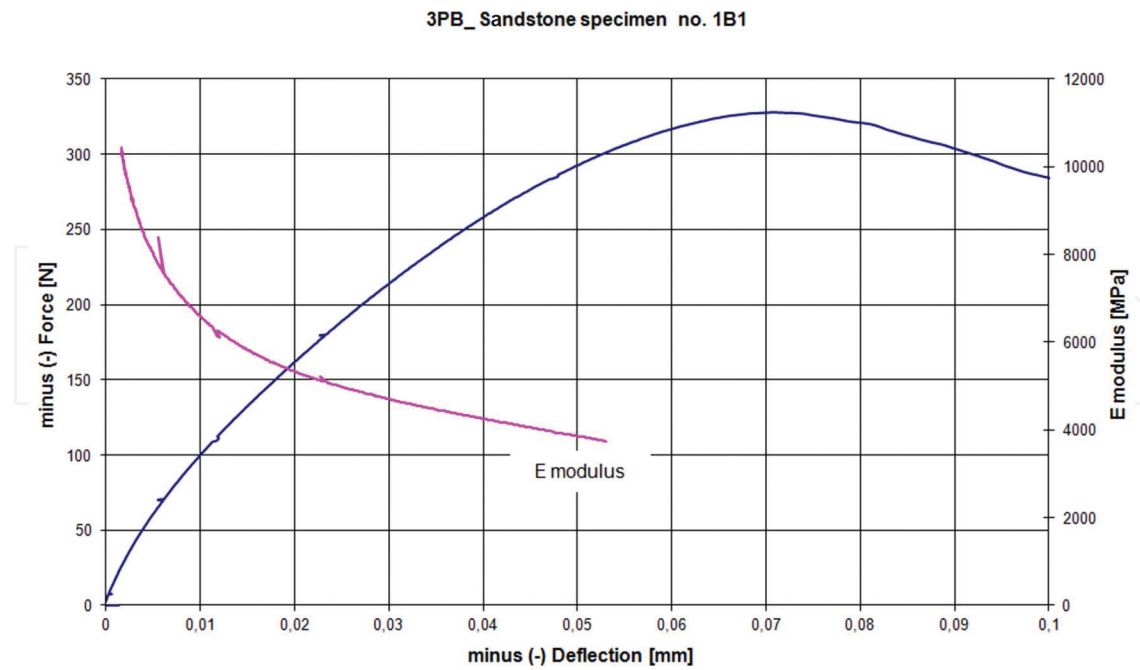
Figure 16. Loading force-deflection diagram during three-point bending testing and calculated modulus of elasticity.

In the study on consolidation effects influencing crack propagation and toughness, three types of specimens were tested—notched beams without cracks, notch beams with cracks generated by cycling, and notched beams with cracks after consolidation [14]. They were loaded in three-point bending configuration.

The results show that consolidation increased the load-carrying capacity of the cracked sandstone specimens. The reference specimen with the initiation notch attained an average bending strength of 5.05 MPa, the notched specimen with the cycled crack one of 4.56 MPa, and the consolidated specimen one of about 6 MPa.

4. Conclusions

Although it is difficult to generalize the results of the pilot tests described here, they provide important findings for further planning of stone fatigue tests.

The methodology of tension tests using specimens inserted and glued in tubular fixtures is functional and has been verified. However, it is very demanding from the point of view of specimen preparation, and it requires very skilled staff. It can be recommended mainly for special small-series tests. For research requiring tests on a large numbers of specimens, it is necessary to develop some other techniques. However, the pilot tests were successfully completed, and the energies for crack initiation and propagation in the given sandstone have been determined.

The optical DIC method again proved its capacity and its suitability for measurements of a complex deformation field on porous and naturally well-structured surfaces.

The modulus of elasticity may be a good parameter for assessing damage accumulation, though it is difficult to measure on real structures (see **Figure 11**). In the next series of tests, the correlation between the modulus of elasticity and NDT techniques will be studied, especially ultrasonic measurements for possible application in situ.

It follows from **Figure 13** that the first tension load displacement can be approximated very satisfactorily by means of a power function.

The tests with consolidated specimens proved the positive effects of stone impregnation on strength and toughness. All notched and cracked specimens after consolidation with ethyl silicates KSE 100 and KSE 300 and Paraloid B-72 attained values above full profile strength which was tested on identical beams. The KSE 300 consolidation agent attained the best result in the range of 145% as far as strength is concerned and 161% in the toughness value (K_{IC}).

The toughness of untreated notched and cracked specimens reached almost the same values (0.33:0.35 MPa√m), which mean that with such a heterogeneous material, one cannot expect stress concentration factors similar to those of metals.

Acknowledgements

Author details

Martin Šperl* and Miloš Drdácký

*Address all correspondence to: sperl@itam.cas.cz

Institute of Theoretical and Applied Mechanics of the Academy of Sciences of the Czech Republic, Prague, The Czech Republic

References

[1] Drdácký MF. Impact of climate change on building structures. In: Lefèvre RA, Sabbioni C, editors. Climate Change and Cultural Heritage. Scienze e materiali del patrimonio culturale, 10. Bari: EDIPUGLIA, s. r. l.; 2010. pp. 139-153

[2] Beran P, Drdácký M. Influence of temperature changes on stresses in the Triforium tracery of St Vitus' Cathedral in Prague. In: Oñate E, Papadrakakis M, Schrefler B, editors. Proceedings Computational Methods for Coupled Problems in Science and Engineering II Coupled Problems. Barcelona: CIMNE; 2007. pp. 433-436

[3] Ning L, Ping Z, Yunsheng C, Gunter S. Fatigue properties of cracked, saturated and frozen sandstone samples under cyclic loading. International Journal of Rock Mechanics and Mining Sciences. 2003;**40**:145-150

[4] Bagde MN, Petroš MN. Fatigue properties of intact sandstone samples subjected to dynamic uniaxial cyclical loading. International Journal of Rock Mechanics and Mining Sciences. 2005;**42**:237-250

[5] Backers T. Fracture Toughness Determination and Micromechanics of Rock Under Mode I and Mode II Loading. PhD Thesis. Universität Potsdam 2004. Scientific Technical Report STR 05/05, GeoForschungsZentrum Potsdam; 2004. p. 138

[6] Attewell PB, Farmer IW. Fatigue behaviour of rock. International Journal of Rock Mechanics and Mining Sciences and Geomechanics Abstracts. 1973;**10**(1):1-9

[7] Jian-Qing X, De-Xin D, Fu-Liang J, Gen X. Fatigue damage variable and evolution of rock subjected to cyclic loading. International Journal of Rock Mechanics and Mining Science. 2010;**47**:461-468. DOI: 10.1016/j.ijrmms.2009.11.003

[8] Cardani G, Meda A. Marble behaviour under monotonic and cyclic loading in tension. Construction and Building Materials. 2004;**18**:419-424

[9] Lin Q, Labuz JF. Fracture of sandstone characterized by digital image correlation. International Journal of Rock Mechanics and Mining Sciences. 2013;**60**:235-245

[10] Peters WH, Ranson WF. Digital imaging techniques in experimental stress analysis. Optical Engineering. 1982;**21**:427-431

[11] Lucas BD, Kanade T. An iterative image registration technique with an application to stereo vision. In: Proceedings of Imaging Understanding Workshop; 1981. pp. 121-130

[12] Drdácký M, Šperl M, Jandejsek I. Consolidation effects on sandstone toughness. In: Hughes J, Howind T, editors. Proceedings of the 13th Int. Congress on the Deterioration and Conservation of Stone "SCIENCE and ART: A Future for Stone". Vol. 2. Paisley: University of West Scotland; 2016. pp. 687-694

[13] Čechová E, Drdácký M, Frankeová D, Lesák J, Slížková Z, Valach J, et al. Technology Guidelines for Restoration of the XIth Arch of the Charles Bridge in Prague. Research Report of ITAM AS CR. Prague: ITAM; 2010. p. 139

[14] Šperl M, Drdácký M. Non-standard experimental tests of sandstone and its pre-cracking for fracture testing. In: IOP Conference Series: Materials Science and Engineering 379; 2018. DOI: 10.1088/1757-899X/379/1/012029